Combining antibiotics with antivirulence compounds is effective and can reverse selection for antibiotic resistance in *Pseudomonas aeruginosa*

Chiara Rezzoagli[1,2], Martina Archetti[1,2], Michael Baumgartner[3], Rolf Kümmerli[1,2*]

[1]Department of Quantitative Biomedicine, University of Zurich, Zurich, Switzerland

[2]Department of Plant and Microbial Biology, University of Zurich, Zurich, Switzerland

[3] Institute for Integrative Biology, Department of Environmental Systems Science, ETH Zurich, Zurich, Switzerland

Short title: Antibiotic-antivirulence combination therapy against bacterial pathogens

Corresponding author: Rolf Kümmerli, Department of Quantitative Biomedicine, University of Zurich, Winterthurerstrasse 190, 8057 Zurich, Switzerland.

Email: rolf.kuemmerli@uzh.ch / Phone: +41 44 635 48 01.

Abstract

Antibiotics are losing efficacy due to the rapid evolution and spread of resistance. Treatments targeting bacterial virulence factors have been considered as alternatives because they target virulence instead of pathogen viability, and should therefore exert weaker selection for resistance than conventional antibiotics. However, antivirulence treatments rarely clear infections, which compromises their clinical applications. Here, we explore the potential of combining antivirulence drugs with antibiotics against the opportunistic human pathogen *Pseudomonas aeruginosa*. We combined two antivirulence compounds (gallium, a siderophore-quencher, and furanone C-30, a quorum sensing-inhibitor) together with four clinically relevant antibiotics (ciprofloxacin, colistin, meropenem, tobramycin) in 9x9 drug concentration matrices. We found that drug-interaction patterns were concentration dependent, with clinically interesting levels of synergies occurring at intermediate drug concentrations for certain drug pairs. We then tested whether antivirulence compounds are potent adjuvants, especially when treating antibiotic resistant clones. We found that the addition of antivirulence compounds to antibiotics could restore growth inhibition for most antibiotic resistant clones, and even reverse selection for resistance in three drug combination cases. Molecular analyses suggest that selection reversal occurs when resistance mechanisms involve restoration of protein synthesis, but not when efflux pumps are upregulated. Altogether, our work provides a first systematic analysis of antivirulence-antibiotic combinatorial treatments and suggests that such combinations have a high potential to be both effective in treating infections and in limiting the spread of antibiotic resistance.

41 ## Introduction

42 Scientists together with the World Health Organization (WHO) forecast that the rapid
43 evolution and spread of antibiotic resistant bacteria will lead to a world-wide medical
44 crisis [1–3]. Already today, the effective treatment of an increasing number of
45 infectious diseases has become difficult in many cases [4,5]. To avert the crisis,
46 novel innovative approaches that are both effective against pathogens and robust to
47 the emergence and spread of resistance are urgently needed [6,7]. One such
48 approach involves the use of compounds that disarm rather than kill bacteria. These
49 so-called 'antivirulence' treatments should exert weaker selection for resistance
50 compared to classical antibiotics because they simply disable virulence factors but
51 are not supposed to affect pathogen viability [8–10]. However, a downside of
52 antivirulence approaches is that the infection will not necessarily be cleared. This
53 could be particularly problematic for immuno-compromised patients (AIDS, cancer,
54 cystic fibrosis and intensive-care unit patients), whose immune system is conceivably
55 too weak to clear even disarmed pathogens.
56
57 One way to circumvent this problem is to combine antivirulence compounds with
58 antibiotics to benefit from both virulence suppression and effective pathogen removal
59 [6,11]. While a few studies have already considered such combinatorial treatments
60 [12–18], we currently have no comprehensive understanding of how different types of
61 antibiotics and antivirulence drugs interact, whether interactions are predominantly
62 synergistic or antagonistic, and how combinatorial treatments affect the spread of
63 antibiotic resistance. Here, we tackle these open issues by combining four different
64 classes of antibiotics with two antivirulence compounds, in 9x9 drug concentration

matrixes, as treatments against the opportunistic human pathogen *Pseudomonas aeruginosa*.

P. aeruginosa is one of the ESKAPE pathogens with multi-drug resistant strains spreading worldwide and infections becoming increasingly difficult to treat [19,20]. In addition to its clinical relevance, *P. aeruginosa* has become a model system for antivirulence research. Several antivirulence compounds targeting either the species' quorum sensing (QS) [21–23] or siderophore-mediated iron uptake systems [24–27] have been proposed. While QS is a cell-to-cell communication system that controls the expression of multiple virulence factors including exo-proteases, biosurfactants and toxins, siderophores are secondary metabolites important for the scavenging of iron from host tissue. For our experiments, we chose antivirulence compounds that target these two different virulence mechanisms: furanone C-30, an inhibitor of the LasR QS-system [12,21], and gallium, targeting the iron-scavenging pyoverdine and iron-metabolism [24,26,28–32].

Furanone C-30 is a synthetic, brominated furanone, which includes the same lactone ring present in the acylhomoserine lactones (AHL) QS molecules of *P. aeruginosa* [33]. As a consequence, it can disrupt QS-based communication by antagonistically competing with the AHLs molecules for binding to the main QS (LasR) receptor [34]. Gallium is an iron mimic whose ionic radius and coordination chemistry is comparable to ferric iron, although its redox properties are different. Specifically, gallium cannot be reduced and thereby irreversibly binds to siderophores and hinders siderophore-mediated iron uptake [24,26].

We combined the two antivirulence compounds with four clinically relevant antibiotics (ciprofloxacin, colistin, meropenem, and tobramycin), which are widely used against *P. aeruginosa* [35]. In a first step, we measured treatment effects on bacterial growth and virulence factor production for all eight drug combinations for 81 concentration combinations each. In a second step, we applied the Bliss independence model to calculate the degree of synergy or antagonism to obtain comprehensive interaction maps for all combinations both for growth and virulence factor production. Next, we selected for antibiotic resistant clones and tested whether the addition of antivirulence compounds as adjuvants can re-potentiate antibiotics and reverse selection for resistance. Finally, we sequenced the genomes of the evolved antibiotic resistant clones to examine the genetic basis that drive the observed patterns of cross-resistance and resistance reversal.

Results

PAO1 dose-response curves to antibiotics and antivirulence compounds

In a first experiment, we determined the dose-response curve of PAO1 to each of the four antibiotics (Figure 1) and the two anti-virulence compounds (Figure 2) in our experimental media. We found that the dose-response curves for antibiotics followed sigmoid functions (Figure 1), characterised by (i) a low antibiotic concentration range that did not inhibit bacterial growth, (ii) an intermediate antibiotic concentration range that significantly reduced bacterial growth, and (iii) a high antibiotic concentration range that completely stalled bacterial growth.

Similar dose-response curves were obtained for gallium (quenching pyoverdine) and furanone C-30 (inhibiting protease production) in the respective media where the two

115 virulence factors are important for growth (Figure 2). Crucially, the dose-response
116 curves shifted to the right (extending phase (i)) when we repeated the experiment in
117 media, where the virulence factors are not needed for growth (i.e. iron-rich media for
118 pyoverdine, and protein digest media for proteases). This shows that there is a
119 window of concentrations where growth inhibition is caused by virulence factor
120 quenching alone. Conversely, high concentrations of antivirulence compounds seem
121 to have additional off-target effects curbing growth.
122
123 **Interaction maps of antibiotic-antivirulence drug combinations**
124 *General patterns*. From the dose-response curves, we chose 9 concentrations for
125 each drug to cover the entire trajectory, from no to intermediate to high growth
126 inhibition. We then combined antibiotics with antivirulence compounds in a 9x9
127 concentration matrix and measured the dose-response curve for every single drug
128 combination for both growth and virulence factor production (Figure 3). At the
129 qualitative level, independent drug effects would cause a symmetrical downshift of
130 the dose-response curve with higher antivirulence compound concentrations
131 supplemented. We indeed noticed symmetrical downshifts for many dose-response
132 curves (Figure 3), but there were also clear cases of non-symmetrical shifts,
133 indicating synergy or antagonism between drugs. When using the Bliss model to
134 quantify these effects, we found patterns of synergy and antagonism for both growth
135 and virulence factor inhibition across the concentration matrices for all drug
136 combinations (Figure 4).
137
138 *Gallium-antibiotic combinations*. Gallium combined with ciprofloxacin or colistin had
139 mostly independent effects on bacterial growth (i.e. weak or no synergy/antagonism)

(Figures 4A+B). With regard to the inhibition of pyoverdine production, both drug combinations showed a tendency towards stronger synergy at intermediate drug concentrations (Figure 4E+F). For gallium-meropenem combinations, we observed mostly independent interactions for growth and pyoverdine inhibition, with small hotspots of antagonism (for growth) and synergy (for siderophore inhibition) existing at intermediate drug concentrations (Figure 4C+G). Finally, for gallium-tobramycin combinations there were relatively strong synergistic interactions for both growth (Figure 4D) and pyoverdine inhibition (Figure 4H) at intermediate drug concentrations.

Furanone-antibiotic combinations. For furanone-ciprofloxacin combinations, we found relatively strong antagonistic interactions with regard to growth inhibition (Figure 4I), whereas effects on protease inhibition were mostly independent (Figure 4M). In contrast, for furanone-colistin combinations we observed strong synergistic drug interactions especially for intermediate and higher concentrations of the antivirulence compound for growth and protease inhibition (Figure 4J+N). Furanone-meropenem, on the other hand, interacted mostly antagonistically with regard to growth and protease inhibition (Figure 4K+O). Conversely, for furanone-tobramycin combinations there were pervasive patterns of synergy across the entire drug combination range for growth and virulence factor inhibition (Figure 4L+P).

Do the degrees of synergy for growth and virulence factor inhibition correlate? As the combinatorial treatments affect both growth and virulence factor production, we examined whether the degrees of synergy correlate between the two traits (Supplementary Figure S1). For gallium-antibiotic combinations, we found no

correlations for ciprofloxacin and meropenem, but positive associations for colistin and tobramycin (Pearson correlation coefficient; ciprofloxacin: $r = 0.09$, $t_{79} = 0.85$, $p = 0.394$; colistin: $r = 0.69$, $t_{79} = 8.51$, $p < 0.001$; meropenem: $r = 0.17$, $t_{79} = 1.53$, $p = 0.130$; tobramycin: $r = 0.58$, $t_{79} = 6.39$, $p < 0.001$). For furanone-antibiotic combinations, there were strong positive correlations between the levels of synergy for the two traits for all drug combinations (ciprofloxacin: $r = 0.34$, $t_{79} = 3.22$, $p = 0.002$; colistin: $r = 0.96$, $t_{79} = 32.50$, $p < 0.001$; meropenem: $r = 0.87$, $t_{79} = 15.48$, $p < 0.001$; tobramycin: $r = 0.75$, $t_{79} = 10.16$, $p < 0.001$).

Antivirulence compounds can restore growth inhibition of antibiotic resistant strains

In a next step, we asked whether antivirulence compounds could be used as adjuvants to suppress the growth of antibiotic resistant clones. To address this question, we first experimentally selected and isolated antibiotic resistant clones (AtbR, see methods for details). We then subjected these AtbR clones to antibiotic and combinatorial treatments and compared their growth relative to the ancestral antibiotic-sensitive wildtype. As expected, AtbR clones grew better than the wildtype under antibiotic treatment alone (two-sample t-tests, $-25.9 \leq t_{7\text{-}16} \leq -2.27$, $p < 0.05$ for all treatments). When adding anti-virulence compounds to the antibiotics, we found that growth inhibition of the AtbR clones was restored in seven out of eight drug combinations (Figure 5A). Overall, there were four different inhibition patterns: the addition of antivirulence compounds either (i) did not affect the growth of the antibiotic resistant strain (one case: ciprofloxacin-furanone); (ii) only fully restored growth inhibition at higher anti-virulence compound concentration (five cases: all four combinations with gallium and colistin-furanone); (iii) restored growth inhibition at low

but not high anti-virulence compound concentration (one case: meropenem-furanone); or (iv) inhibited growth more than in the antibiotic sensitive wildtype (one case: tobramycin-furanone).

Specific drug combinations can reverse selection for antibiotic resistance

We then investigated whether the addition of an antivirulence compound to an antibiotic treatment can influence the spread of AtbR clones in populations of susceptible cells (Figure 5B). Our competition assays revealed that AtbR clones lost against the susceptible wildtype in the absence of antibiotics, confirming that antibiotic resistance is costly (one sample t-tests, $-54.16 \leq t_7 \leq -2.36$, $p \leq 0.050$ for all comparisons). Conversely, AtbR clones always experienced a significant fitness advantage compared to the wildtype under antibiotic treatment (one sample t-test, $3.05 \leq t_7 \leq 12.80$, $p < 0.01$ for all combinations). The addition of antivirulence compounds to the antibiotic treatment had variable and combination-specific effects on the fitness of AtbR clones, which included: (i) three cases where anti-virulence compound addition did not affect the fitness advantage of the AtbR clones (ciprofloxacin-gallium, ciprofloxacin-furanone and colistin-furanone); (ii) two cases where the antivirulence adjuvant further potentiated the spread of AtbR clones (colistin-gallium and meropenem-furanone); and (iii) three cases where the adjuvant reversed selection for antibiotic resistance and thereby hindered the spread of AtbR clones (meropenem-gallium, tobramycin-gallium and tobramycin-furanone). Detailed information on statistical analysis for Figure 5B is reported in Supplementary Table S1.

Drug synergy does not predict selection against antibiotic resistance

We examined whether drug interactions, ranging from antagonism to synergy (Figure 4) correlate with the relative fitness of the AtbR clones in competition with the antibiotic sensitive wildtype. However, we found no support for such associations (Supplementary Figure S2, ANOVA, growth: $F_{1,48} = 0.65$, $p = 0.422$; virulence factor: $F_{1,48} = 3.10$, $p = 0.082$), but instead observed that variation in fitness patterns was explained by specific drug combinations (antivirulence-antibiotic interaction: $F_{3,48} = 15.76$, $p < 0.0001$).

Genetic bases of experimentally evolved antibiotic resistance

The whole-genome sequencing of the experimentally evolved AtbR clones revealed a small number of SNPs and INDELs, which are known to be associated with resistance to the respective antibiotics (Table 1). The AtbR clone resistant to ciprofloxacin had mutations in *gyrB*, a gene encoding the DNA gyrase subunit B, the direct target of the antibiotic [36]. In addition, we identified an 18-bp deletion in the *mexR* gene, encoding a multidrug efflux pump repressor [37]. The two AtbR clones resistant to colistin had different mutations in the same target gene *phoQ* (a non-synonymous SNP in one clone versus a 1-bp insertion in addition to a non-synonymous SNP in the other clone). PhoQ is a regulator of the LPS modification operon and mutations in this gene represent the first step in the development of high-level colistin resistance [38]. One AtbR clone resistant to meropenem had a non-synonymous SNP in the coding sequence of *mpl.* This gene encodes a murein tripeptide ligase, which contributes to the overexpression of the beta-lactamase precursor gene *ampC* [39]. The other AtbR clone resistant to meropenem had mutations in three different genes, which can all be linked to antibiotic resistance mechanisms: we found (i) one non-synonymous SNP in *parR*, which encodes a two

component response regulator involved in several resistance mechanisms, including drug efflux, porin loss and LPS modification [40]; (ii) 7 mutations in the *PA1874* gene, which encodes an efflux pump [41]; (iii) one non-synonymous SNP in *nalD*, encoding the transcriptional regulator NalD, which regulates the expression of drug-efflux systems [42,43]. Both AtbR clones resistant to tobramycin had non-synonymous SNPs in *fusA1*. This gene encodes the elongation factor G, a key component of the translational machinery. Although aminoglycosides do not directly bind to the elongation factor G and the complete resistance mechanisms is still unknown, mutations in *fusA1* are associated with high resistance to tobramycin and are often found in clinical isolates [44,45].

Discussion

In this study, we systematically explored the effects of combining antibiotics with antivirulence compounds as a potentially promising strategy to fight susceptible and antibiotic resistant opportunistic human pathogens. Specifically, we combined four different antibiotics (ciprofloxacin, colistin, meropenem, tobramycin) with two antivirulence compounds (gallium targeting siderophore-mediated iron uptake and furanone C-30 targeting the quorum sensing communication system) in 9x9 drug interaction matrices against the bacterium *P. aeruginosa* as a model pathogen. Our heat maps reveal drug-combination specific interaction patterns. While colistin and tobramycin primarily interacted synergistically with the antivirulence compounds, independent and antagonistic interactions occurred for ciprofloxacin and meropenem in combination with the antivirulence compounds (Figures 3+4). We then used antivirulence compounds as adjuvants and observed that they can restore growth inhibition of antibiotic resistant clones in seven out of eight cases (Figure 5A). Finally,

we performed competition assays between antibiotic resistant and susceptible strains under single and combinatorial drug treatments and found that antivirulence compounds can reverse selection for antibiotic resistance in three out of eight cases (Figure 5B). Our results identify antibiotic-antivirulence combinations as a potentially powerful tool to efficiently treat infections of troublesome nosocomial pathogens such as *P. aeruginosa*. Particularly, tobramycin-antivirulence combinations emerged as the top candidate treatments because: (i) drugs interacted synergistically both with regard to growth and virulence factor inhibition; (ii) the antivirulence compounds re-potentiated tobramycin when treating antibiotic resistant clones; and (iii) antivirulence compounds reversed selection for tobramycin resistance.

Drug synergy is desirable from a clinical perspective because it allows to use lower drug concentrations, thereby minimizing side effects while maintaining treatment efficacy [46,47]. In this context, a number of studies have examined combinations of antibiotics and antivirulence compounds targeting various virulence factors including quorum sensing, iron uptake, and biofilm formation in *P. aeruginosa* [12,13,15–18,22,48–51]. While these studies typically used a handful of concentration combinations and used qualitative measures of synergy, we here present a comprehensive quantitative interaction maps for these two classes of drugs. A key insight of these interaction maps is that specific drug combinations cannot simply be classified as either synergistic or antagonistic. Instead, drug interactions are concentration dependent with most parts of the interaction maps being characterized by independent effects interspersed with hotspots of synergy or antagonism. The strongest effects of synergy and antagonism are often observed at intermediate drug

289 concentrations, which is, in the case of synergy, ideal for developing combinatorial
290 therapies that maximise treatment efficacy while minimizing toxicity for the patient.
291
292 While drug antagonism is considered undesirable from a clinical perspective, work on
293 antibiotic combination therapies has revealed that antagonistic interactions can inhibit
294 the spread of antibiotic resistance [52–54]. The reason behind this phenomenon is
295 that when two drugs antagonize each other, becoming resistant to one drug will
296 remove the antagonistic effect on the second drug, such that the combination
297 treatment will be more effective against the resistant clones [52]. We suspected that
298 such effects might also occur for antagonistic antibiotic-antivirulence treatments.
299 While we indeed observed that combination therapy can reverse selection for
300 resistance in certain cases (Figure 5B), there was no evidence that this effect
301 correlated with the type of drug interaction (Supplementary Figure S2). A possible
302 explanation for the lack of any association is that the antagonism between antibiotics
303 and antivirulence compounds was quite moderate. In contrast, previous work used
304 an extreme case of antagonism, where the effect of one drug was almost completely
305 suppressed in the presence of the second drug [52,54].
306
307 We propose that it is rather the underlying molecular mechanism and not the
308 direction of drug interaction that determines whether selection for antibiotic
309 resistance is reversed or potentiated. For instance, any resistance mechanism that
310 reduces antibiotic entry or increases its efflux could conceivably induce cross-
311 resistance to antivirulence compounds, which should in turn potentiate and not
312 reverse selection for antibiotic resistance. This phenomenon could explain the
313 patterns observed for furanone in combination with ciprofloxacin, colistin and

meropenem, where our sequencing analysis revealed mutations in genes regulating efflux pumps, porins and membrane lipopolysaccharide modifications (Table 1). Since furanone needs to enter the cells to become active, these mutations, known to confer resistance to antibiotics [37,38,41], likely also induce resistance to furanone [55].

Alternatively, competitive interactions between resistant and sensitive pathogens over common resources could compromise the spread of drug resistance, as shown for malaria parasites [56]. In our case, it is plausible to assume that antibiotic resistant clones are healthier than susceptible cells and might therefore produce higher amounts of pyoverdine and proteases under antivirulence treatment. Since these virulence factors are secreted and shared between cells, antibiotic resistant clones take on the role of cooperators: they produce costly virulence factors that are then shared with and exploited by the susceptible cells [26,57,58]. This scenario could apply to tobramycin-gallium/furanone combinations, where resistant clones had mutations in *fusA1* known to be associated with the restoration of protein synthesis [44]. Similar social effects could explain selection reversal in the case of meropenem-gallium combination. Here, the meropenem resistant clone has mutation in *mpl*, which can trigger the overexpression of the β-lactamase *ampC* resistance mechanism [39]. Since β-lactamase enzyme secretion and extracellular antibiotic degradation is itself a cooperative behaviour [59], it could together with the virulence factor sharing described above compromise the spread of the resistant clone. Clearly, all these explanations remain speculative and further studies are required to understand the molecular and evolutionary basis of reversed selection for resistance.

In summary, drug combination therapies are gaining increased attention as more sustainable strategies to treat infections, limiting the spread of antibiotic resistance [60–63]. They are already applied to a number of diseases, including cancer [64], HIV [65] and tuberculosis infections [66]. Here we probed the efficacy and evolutionary robustness of antibiotics combined with anti-virulence compounds. This is an interesting combination because antibiotic treatments alone face the problem of rapid resistance evolution, whereas antivirulence drugs are evolutionarily more robust but can only disarm and not eliminate pathogens. Combinatorial treatments seem to bring the strengths of the two approaches together: efficient removal of bacteria by the antibiotics combined with disarming and increased evolutionary robustness of the antivirulence compounds. While our findings are promising and could set the stage for a novel class of combinatorial treatments, there are still many steps to take to bring our approach to the clinics. First, it would be important to quantify the rate of resistance evolution directly under the combinatorial treatments to test whether drug combination itself slows down resistance evolution [60]. Second, the various antibiotic-antivirulence combinations must be tested in relevant animal host models, as host conditions including the increased spatial structure inside the body can affect the competitive dynamics between strains, potentially influencing the outcome of the therapy [67,68]. Finally, the observed patterns of drug synergy and reversed selection for resistance are concentration dependent (Figure 4-5), thus requiring detailed research on drug delivery and the pharmacodynamics and pharmacokinetics of combination therapies [54].

Materials and methods

Bacterial strains

For all our experiments, we used *P. aeruginosa* PAO1 (ATCC 15692). In addition to the wildtype PAO1, we further used two isogenic variants tagged with either a constitutively expressed GFP or mCherry fluorescent protein. Both fluorescently tagged strains were directly obtained from the wildtype PAO1 using the miniTn7-system to chromosomally integrate a single stable copy of the marker gene, under the strong constitutive Ptac promoter, at the *att*Tn7 site [69]. The gentamycin resistance cassette, required to select for transformed clones, was subsequently removed using the pFLP2-encoded recombinase [69]. Antibiotic resistant clones used for competition assays were generated through experimental evolution and are listed in Table 1 together with their respective mutations.

Media and growth conditions

For all experiments, overnight cultures were grown in 8 ml Lysogeny broth (LB, Sigma Aldrich, Switzerland) in 50 ml Falcon tubes, incubated at 37°C, 220 rpm for 18 hours. We washed overnight cultures with 0.8% NaCl solution and adjusted them to OD_{600} = 1 (optical density at 600 nm). Bacteria were further diluted to a final starting OD_{600} = 10^{-3} for all experiments. We used two different media, where the targeted virulence factors (pyoverdine or protease) are important. For pyoverdine, we used iron-limited CAA (CAA+Tf) [0.5% casamino acids, 5 mM $K_2HPO_4 \cdot 3H_2O$, 1 mM $MgSO_4 \cdot 7H_2O$], buffered at neutral pH with 25 mM HEPES buffer and supplemented with 100 µg/ml human apo-transferrin to chelate iron and 20 mM $NaHCO_3$ as a co-factor. As an iron-rich control medium, we used CAA supplemented with 25 mM HEPES and 20 µM $FeCl_3$, but without apo-transferrin and 20 mM $NaHCO_3$ to create conditions that do not require pyoverdine for growth [70].

For QS-regulated proteases, we used casein medium (CAS) [0.5% casein, 5 mM $K_2HPO_4 \cdot 3H_2O$, 1 mM $MgSO_4 \cdot 7H_2O$], supplemented with 25 mM HEPES buffer and 0.05% CAA. In this medium, proteases are required to digest the casein. A small amount of CAA was added to allow cultures to have a growth kick start prior to protease secretion [71]. As a control, we used CAA supplemented with 25 mM HEPES buffer, a medium in which proteases are not required. All chemicals were purchased from Sigma Aldrich, Switzerland. The CAS medium is intrinsically turbid due to the poor solubility of casein, which can interfere with the growth kinetics measured via optical density (Supplementary Figure S3A). To solve this issue, we used mCherry fluorescence intensity as a reliable proxy for growth in CAS (Supplementary Figure S3B-C).

Single drug growth and virulence factor inhibition curves

To determine the activity range of each antibiotic (ciprofloxacin, colistin, meropenem, tobramycin) and antivirulence drug (gallium as $GaNO_3$ and furanone C-30), we subjected PAO1 bacterial cultures to two different 7-step serial dilutions for each antibacterial. Ciprofloxacin: 0-4 µg/ml; colistin: 0-0.4 µg/ml in CAA+Tf and 0-20 µg/ml in CAS; meropenem: 0-14 µg/ml; tobramycin: 0-8 µg/ml; gallium: 0-200 µM; furanone C-30: 0-390 µM. All antibacterials were purchased from Sigma Aldrich, Switzerland. Overnight cultures were prepared and diluted as explained above and then added into 200 µl of media on 96-well plates with six replicates for each drug concentration. Plates were incubated statically at 37°C and growth was measured either as OD_{600} (in CAA+Tf) or mCherry fluorescence (excitation 582 nm, emission 620 nm in CAS) after 48 hours using a Tecan Infinite M-200 plate reader (Tecan Group Ltd., Switzerland). Control experiments (Supplementary Figure S4) confirmed that

endpoint OD_{600} or mCherry measurements showed strong linear correlations ($0.858 < R^2 < 0.987$) with the growth integral (area under the growth curve), which is a good descriptor of the overall inhibitory effects covering the entire growth period [72].

At this time point, we further quantified pyoverdine production through its natural fluorescence (excitation 400 nm, emission 460 nm) and protease production in the cell-free supernatant using the protease azocasein assay (adapted from [73] shortening incubation time to 30 min). The two metals, gallium and bromine (in Furanone C-30), alter the fluorescence levels of pyoverdine and mCherry in a concentration dependent manner. To account for this effect, we established calibration curves and corrected all fluorescence measures accordingly (as described in Supplementary Figure S5).

Antibiotic-antivirulence combination assays

From the single drug dose-response curves, we chose for each drug nine concentrations (including no drugs) to cover the entire activity range in each medium including no, intermediate and strong inhibitory growth effects on PAO1. (Supplementary Table S2). We then combined these drug concentrations in a 9x9 matrix for each of the eight antibiotic-antivirulence pairs, and repeated the growth experiment for all combinations in six-fold replication, exactly as described above. After 48 hours of incubation, we measured growth and virulence factor production following the protocols described above.

Synergy degree of drug-combinations

We used the Bliss independence model to calculate the degree of synergy (S), for both growth and virulence factor inhibition, for each of the antibiotic-antivirulence combinations [74–76]. We used the formula $S = f_{X,0} \cdot f_{0,Y} - f_{X,Y}$, where $f_{X,0}$ is the growth (or virulence factor production) level measured under antibiotic exposure at concentration X; $f_{0,Y}$ is the growth (or virulence factor production) level measured under antivirulence exposure at concentration Y; and $f_{X,Y}$ is the growth (or virulence factor production) level measured under the combinatorial treatment at concentrations X and Y. If $S = 0$ then the two drugs act independently. Conversely, $S < 0$ indicates antagonistic drug interactions, while $S > 0$ indicates synergy.

Experimental evolution under antibiotic treatment

To select for antibiotic resistant clones, we exposed overnight cultures of PAO1 wildtype (initial $OD_{600} = 10^{-4}$) to each of the four antibiotics in LB medium (antibiotic concentrations, ciprofloxacin: 0.15 µg/ml; colistin: 0.5 µg/ml; meropenem: 0.8 µg/ml; tobramycin: 1 µg/ml) in six-fold replication. These antibiotic concentrations initially caused a 70-90% reduction in PAO1 growth compared to untreated cultures, conditions that imposed strong selection for the evolution of resistance. The evolution experiment ran for seven days, whereby we diluted bacterial cultures and transferred them to fresh medium with the respective treatment with a dilution factor of 10^{-4}, every 24 hours. At the end of each growth cycle, we measured growth (OD_{600}) of the evolving lineages using a SpectraMax® Plus 384 plate reader (Molecular Devices, Switzerland).

Phenotypic and genetic characterization of resistance

462 Following experimental evolution, we screened the evolved lines for the presence of
463 antibiotic resistant clones. For each antibiotic we plated four evolved lines on LB
464 plates and isolated single clones, which we then exposed in liquid culture to the
465 antibiotic concentration they experienced during experimental evolution. Among
466 those that showed growth restoration (compared to the untreated wildtype), we
467 picked two random clones originating from different lineages per antibiotic for further
468 analysis. We had to adjust our sampling design in two cases. First, only one
469 population survived our ciprofloxacin treatment and thus only one resistant clone
470 could be picked for this antibiotic. Second, clones evolved under colistin treatment
471 grew very poorly in CAS medium and therefore we included an experimentally
472 evolved colistin resistant clone from a previous study, which did not show
473 compromised growth in CAS (see [73] for a description on the experimental
474 evolution). Altogether, we had seven clones for which we re-established the drug-
475 response curves (Supplementary Figure S6) in either CAA+Tf or CAS (one clone per
476 antibiotic was allocated to one of the two media, except for ciprofloxacin).
477
478 We further isolated the genomic DNA of the selected evolved antibiotic resistant
479 clones and sequenced their genomes. We used the GenElute Bacterial Genomic
480 DNA kit (Sigma Aldrich) for DNA isolation. DNA concentrations were assayed using
481 the Quantifluor dsDNA sample kit (Promega, Switzerland). Samples were sent to the
482 Functional Genomics Center Zurich for library preparation (TruSeq DNA Nano) and
483 sequencing on the Illumina MiSeq platform with v2 reagents and pair-end 150 bp
484 reads. In a first step, we mapped the sequences of our ancestral wildtype PAO1
485 strain (ENA accession number: ERS1983671) to the *Pseudomonas aeruginosa*
486 PAO1 reference genome (NCBI accession number: NC_002516) with snippy

(https://github.com/tseemann/snippy) to obtain a list with variants that were already present at the beginning of the experiment. Next, we quality filtered the reads of the evolved clones with trimmomatic [77], mapped them to the reference genome and called variants using snippy. Detected variants were quality filtered and variants present in the ancestor strain were excluded from the dataset using vcftools [78]. The mapping files generated in this study are deposited in the European Nucleotide Archive (ENA) under the study accession number PRJEB32766.

Competition experiments between sensitive and resistant clones

To examine the conditions under which antibiotic resistant clones can spread, we competed the sensitive wildtype PAO1 (tagged with GFP) against the experimentally evolved antibiotic resistant clones (Table 1) under five different conditions: (i) no drug treatment; (ii) antibiotic alone; (iii)-(v) antibiotic combined with three different concentrations of the antivirulence compound. Antibiotic concentrations are listed in the Supplementary Table S3, while antivirulence concentrations were as follows, gallium: 1.56 µM (low), 6.25 µM (medium), 12.5 µM (high); furanone: 6.3 µM (low), 22.8 µM (medium), 51.4 µM (high). Bacterial overnight cultures were prepared and diluted as described above. Competitions were initiated with a mixture of 90% sensitive wildtype cells and 10% resistant clones to mimic a situation where resistance is still relatively rare. Mixes alongside with monocultures of all strains were inoculated in either 200 µl of CAA+Tf or CAS under all the five treatment regimes. We used flow cytometry to assess strain frequency prior and after a 24 hours competition period at 37°C static (Supplementary Figure S7). Specifically, bacterial cultures were diluted in 1X phosphate buffer saline (PBS, Gibco, ThermoFisher, Switzerland) and frequencies were measured with a LSRII Fortessa cell analyzer (BD

512 Bioscience, Switzerland. GFP channel, laser: 488 nm, mirror: 505LP, filter: 530/30;
513 side and forward scatter: 200 V threshold; events recorded with CS&T settings) at
514 the Cytometry Facility of the University of Zurich. We recorded 50'000 events before
515 competitions and used a high-throughput sampler device (BD Bioscience) to record
516 all events in a 5 µl-volume after competition. Since antibacterials can kill and thereby
517 quench the GFP signal in tagged cells, we quantified dead cells using the propidium
518 iodide (PI) stain (2 µl of 0.5 mg/ml solution) with flow cytometry (for PI fluorescence:
519 laser: 561 nm, mirror: 600LP, filter: 610/20).
520
521 We used the software FlowJo (BD Bioscience) to analyse data from flow cytometry
522 experiments. We followed a three-step gating strategy: (i) we separated bacterial
523 cells from media and noise background by using forward and side scatter values as a
524 proxy for particle size; (ii) within this gate, we then distinguished live from dead cells
525 based on the PI staining; (iii) finally, we separated live cells into either GFP positive
526 and negative populations. Fluorescence thresholds were set using appropriate
527 control samples: isopropanol-killed cells for PI positive staining and untagged-PAO1
528 cells for GFP-negative fluorescence. We then calculated the relative fitness of the
529 antibiotic resistant clone as $\ln(v) = \ln\{[a_{24}\times(1-a_0)]/[a_0\times(1-a_{24})]\}$, where a_0 and a_{24} are
530 the frequencies of the resistant clone at the beginning and at the end of the
531 competition, respectively [79]. Values of $\ln(v) < 0$ or $\ln(v) > 0$ indicate whether the
532 frequency of antibiotic resistant clones decreased or increased relative to the
533 sensitive PAO1-GFP strain. To check for fitness effects caused by the fluorescent
534 tag, we included a control competition, where we mixed PAO1-GFP with the
535 untagged PAO1 in a 9:1 ratio for all treatment conditions. We noted that high drug
536 concentrations significantly curbed bacterial growth, which reduced the number of

537 events that could be measured with flow cytometry. This growth reduction increased
538 noise relative to the signal, leading to an overestimation of the GFP-negative
539 population in the mix. To correct for this artefact, we established calibration curves
540 (described by asymptotic functions, Supplementary Table S2) for how the relative
541 fitness of PAO1-untagged varies as a function of cell density in control competitions
542 with PAO1-GFP.
543
544 **Statistical analysis**
545 All statistical analyses were performed with RStudio v. 3.3.0 [80]. We fitted individual
546 dose response curves with either log-logistic or Weibull functions using the drc
547 package [81], while dose response curves under combination treatment were fitted
548 using spline functions. We used Pearson correlation coefficients to test for significant
549 associations between the degree of synergy in growth and virulence factor inhibition.
550 We used Welch's two-sample t-test to compare growth between the sensitive
551 wildtype PAO1 and the resistant clones under antibiotic treatment. To compare the
552 relative fitness of resistant clones to the reference zero line, we used one sample t-
553 tests. Finally, we used analysis of variance (ANOVA) to compare: (a) the growth of
554 sensitive and resistant clones across combination treatments; (b) the relative fitness
555 of evolved clones across treatments, and (c) whether the outcome of the competition
556 experiment is associated with the degree of synergy of the drug combinations. Where
557 necessary, p-values were adjusted for multiple comparisons using the false discovery
558 rate method.

Acknowledgments

We thank Roland Regös and Désirée Bäder for advice on the Bliss model; Alex Hall, Roland Regös and Frank Schreiber for comments on the manuscripts; Ingrid Mignot and David Wilson for experimental support; Selina Niggli, Priyanikha Jayakumar and the Flow Cytometry Facility (University of Zurich) for support with flow cytometry experiments; and the Functional Genomics Center Zurich for technical support with the strain sequencing.

Funding

This project has received funding from the Swiss National Science Foundation (grant no. 31003A_182499 to RK) and the European Research Council (ERC) under the European Union's Horizon 2020 research and innovation programme (grant agreement no. 681295 to RK).

Competing Interests

The authors have no competing interests to declare.

References

1. Rossolini GM, Arena F, Pecile P, Pollini S. Update on the antibiotic resistance crisis. Curr Opin Pharmacol. Elsevier Ltd; 2014;18: 56–60. doi:10.1016/j.coph.2014.09.006

2. World Health Organization (WHO). Antimicrobial resistance: Global Health Report on Surveillance [Internet]. Bulletin of the World Health Organization. 2014. doi:10.1007/s13312-014-0374-3

3. O'Neill J. Antimicrobial Resistance: Tackling a crisis for the health and wealth of nations. Review on Antimicrobial Resistance. London; 2014. doi:10.1038/510015a

4. Tacconelli E, Carrara E, Savoldi A, Harbarth S, Mendelson M, Monnet DL, et al. Discovery, research, and development of new antibiotics: the WHO priority list of antibiotic-resistant bacteria and tuberculosis. Lancet Infect Dis. Elsevier; 2018;18: 318–327. doi:10.1016/S1473-3099(17)30753-3

5. Laxminarayan R, Matsoso P, Pant S, Brower C, Rottingen J-A, Klugman K, et al. Access to effective antimicrobials: a worldwide challenge. Lancet. England; 2016;387: 168–175. doi:10.1016/S0140-6736(15)00474-2

6. Dickey SW, Cheung GYC, Otto M. Different drugs for bad bugs: antivirulence strategies in the age of antibiotic resistance. Nat Rev Drug Discov. 2017;16: 1–15. doi:10.1038/nrd.2017.23

7. Brown D. Antibiotic resistance breakers: can repurposed drugs fill the antibiotic discovery void? Nat Rev Drug Discov. 2015;14: 821–832. doi:10.1038/nrd4675

8. Allen RC, Popat R, Diggle SP, Brown SP. Targeting virulence: can we make evolution-proof drugs? Nat Rev Microbiol. 2014;12: 300–308. doi:10.1038/nrmicro3232

9. Vale PF, Fenton A, Brown SP. Limiting Damage during Infection: Lessons from Infection Tolerance for Novel Therapeutics. PLOS Biol. 2014;12. doi:10.1371/journal.pbio.1001769

10. Vale PF, McNally L, Doeschl-Wilson A, King KC, Popat R, Domingo-Sananes MR, et al. Beyond killing. Evol Med Public Heal. 2016;2016: 148–157. doi:10.1093/emph/eow012

11. Ternent L, Dyson RJ, Krachler AM, Jabbari S. Bacterial fitness shapes the population dynamics of antibiotic-resistant and -susceptible bacteria in a model of combined antibiotic and anti-virulence treatment. J Theor Biol. Elsevier; 2015;372: 1–11. doi:10.1016/j.jtbi.2015.02.011

12. Hentzer M, Wu H, Andersen JB, Riedel K, Rasmussen TB, Bagge N, et al. Attenuation of Pseudomonas aeruginosa virulence by quorum sensing inhibitors. EMBO J. 2003;22: 3803–3815. doi:10.1093/emboj/cdg366

13. Banin E, Lozinski A, Brady KM, Berenshtein E, Butterfield PW, Moshe M, et al. The potential of desferrioxamine-gallium as an anti-*Pseudomonas* therapeutic agent. Proc Natl Acad Sci U S A. 2008;105: 16761–16766. doi:10.1073/pnas.0808608105

14. Zeng Z, Qian L, Cao L, Tan H, Huang Y, Xue X, et al. Virtual screening for novel quorum sensing inhibitors to eradicate biofilm formation of Pseudomonas aeruginosa. Appl Microbiol Biotechnol. 2008;79: 119–126. doi:10.1007/s00253-008-1406-5

15. Jakobsen TH, Van Gennip M, Phipps RK, Shanmugham MS, Christensen LD, Alhede M, et al. Ajoene, a sulfur-rich molecule from garlic, inhibits genes controlled by quorum sensing. Antimicrob Agents Chemother. 2012;56: 2314–2325. doi:10.1128/AAC.05919-11

16. Michaud G, Visini R, Bergmann M, Salerno G, Bosco R, Gillon E, et al. Overcoming antibiotic resistance in Pseudomonas aeruginosa biofilms using glycopeptide dendrimers. Chem Sci. 2016;7: 166–182. doi:10.1039/c5sc03635f

17. Goss CH, Kaneko Y, Khuu L, Anderson GD, Ravishankar S, Aitken ML, et al. Gallium disrupts bacterial iron metabolism and has therapeutic effects in mice and humans with lung infections. Sci Transl Med. 2018;10: eaat7520.

18. Kirienko DR, Kang D, Kirienko N V. Novel Pyoverdine Inhibitors Mitigate Pseudomonas aeruginosa Pathogenesis. Front Microbiol. 2019;9: 3317.

19. Breidenstein EBM, de la Fuente-Núñez C, Hancock REW. *Pseudomonas aeruginosa*: all roads lead to resistance. Trends Microbiol. 2011;19: 419–426. doi:10.1016/j.tim.2011.04.005

20. Gellatly SL, Hancock REW. Pseudomonas aeruginosa: New insights into pathogenesis and host defenses. Pathog Dis. 2013;67: 159–173. doi:10.1111/2049-632X.12033

21. Hentzer M, Riedel K, Rasmussen TB, Heydorn A, Andersen JB, Parsek MR, et al. Inhibition of quorum sensing in Pseudomonas aeruginosa biofilm bacteria by a halogenated furanone compound Inhibition of quorum sensing in Pseudomonas aeruginosa biofilm bacteria by a halogenated furanone compound. Microbiology. 2002;148: 87–102. doi:10.1099/00221287-148-1-87

22. Rasmussen TB, Bjarnsholt T, Skindersoe ME, Hentzer M, Kristoffersen P, Köte M, et al. Screening for Quorum-Sensing Inhibitors (QSI) by Use of a Novel Genetic System, the QSI Selector. J Bacteriol. 2005;187: 1799 LP-1814. doi:10.1128/JB.187.5.1799-1814.2005

23. Defoirdt T. Quorum-Sensing Systems as Targets for Antivirulence Therapy. Trends Microbiol. Elsevier Ltd; 2018;26: 313–328.

650 doi:10.1016/j.tim.2017.10.005

651 24. Kaneko Y, Thoendel M, Olakanmi O, Britigan BE, Singh PK. The transition
652 metal gallium disrupts *Pseudomonas aeruginosa* iron metabolism and has
653 antimicrobial and antibiofilm activity. J Clin Invest. 2007;117: 877–888.
654 doi:10.1172/JCI30783

655 25. Smith DJ, Lamont IL, Anderson GJ, Reid DW. Targeting iron uptake to control
656 *Pseudomonas aeruginosa* infections in cystic fibrosis. Eur Respir J. 2013;42:
657 1723–36. doi:10.1183/09031936.00124012

658 26. Ross-Gillespie A, Weigert M, Brown SP, Kümmerli R. Gallium-mediated
659 siderophore quenching as an evolutionarily robust antibacterial treatment. Evol
660 Med Public Heal. 2014;2014: 18–29. doi:10.1093/emph/eou003

661 27. Imperi F, Massai F, Facchini M, Frangipani E, Visaggio D, Leoni L, et al.
662 Repurposing the antimycotic drug flucytosine for suppression of *Pseudomonas*
663 *aeruginosa* pathogenicity. Proc Natl Acad Sci U S A. 2013;110: 7458–63.
664 doi:10.1073/pnas.1222706110

665 28. DeLeon K, Balldin F, Watters C, Hamood A, Griswold J, Sreedharan S, et al.
666 Gallium Maltolate Treatment Eradicates *Pseudomonas aeruginosa* Infection in
667 Thermally Injured Mice. Antimicrob Agents Chemother. 2009;53: 1331–1337.
668 doi:10.1128/AAC.01330-08

669 29. Kelson AB, Carnevali M, Truong-Le V. Gallium-based anti-infectives: targeting
670 microbial iron-uptake mechanisms. Curr Opin Pharmacol. 2013;13: 707–716.
671 doi:10.1016/j.coph.2013.07.001

672 30. Bonchi C, Imperi F, Minandri F, Visca P, Frangipani E. Repurposing of gallium-
673 based drugs for antibacterial therapy. BioFactors. 2014;40: 303–312.
674 doi:10.1002/biof.1159

675 31. Hijazi S, Visca P, Frangipani E. Gallium-Protoporphyrin IX Inhibits
676 *Pseudomonas aeruginosa* Growth by Targeting Cytochromes. Front Cell Infect
677 Microbiol. 2017;7: 1–15. doi:10.3389/fcimb.2017.00012
678 32. Hijazi S, Visaggio D, Pirolo M, Frangipani E, Bernstein L, Visca P. Antimicrobial
679 activity of gallium compounds on ESKAPE pathogens. Front Cell Infect
680 Microbiol. 2018;8: 316.
681 33. Manny AJ, Kjelleberg S, Kumar N, de Nys R, Read RW, Steinberg P.
682 Reinvestigation of the sulfuric acid-catalysed cyclisation of brominated 2-
683 alkyllevulinic acids to 3-alkyl-5-methylene-2 (5H)-furanones. Tetrahedron.
684 Elsevier; 1997;53: 15813–15826.
685 34. Manefield M, de Nys R, Kumar N, Read R, Givskov M, Steinberg P, et al.
686 Evidence that halogenated furanones from Delisea pulchra inhibit acylated
687 homoserine lactone (AHL)-mediated gene expression by displacing the AHL
688 signal from its receptor protein. Microbiology. 1999;145 (Pt 2: 283–291.
689 35. Bassetti M, Vena A, Croxatto A, Righi E, Guery B. How to manage
690 Pseudomonas aeruginosa infections. Drugs Context. England; 2018;7: 212527.
691 doi:10.7573/dic.212527
692 36. Rehman A, Patrick WM, Lamont IL. Mechanisms of ciprofloxacin resistance in
693 pseudomonas aeruginosa: New approaches to an old problem. J Med
694 Microbiol. 2019;68: 1–10. doi:10.1099/jmm.0.000873
695 37. Poole K, Neshat S, Heinrichs DE, Zhao Q, Tetro K, Bianco N. Expression of
696 the multidrug resistance operon mexA-mexB-oprM in Pseudomonas
697 aeruginosa: mexR encodes a regulator of operon expression. Antimicrob
698 Agents Chemother. 2018;40: 2021–2028. doi:10.1128/aac.40.9.2021
699 38. Jochumsen N, Paulander W, Jensen RL, Folkesson A, Molin S, Jelsbak L, et

al. The evolution of antimicrobial peptide resistance in Pseudomonas aeruginosa is shaped by strong epistatic interactions. Nat Commun. 2016;7: 13002. doi:10.1038/ncomms13002

39. Tsutsumi Y, Tomita H, Tanimoto K. Identification of Novel Genes Responsible for Overexpression of ampC in Pseudomonas aeruginosa PAO1 . Antimicrob Agents Chemother. 2013;57: 5987–5993. doi:10.1128/aac.01291-13

40. Muller C, Plésiat P, Jeannot K. A Two-Component Regulatory System Interconnects Resistance to Polymyxins, Aminoglycosides, Fluoroquinolones, and beta-Lactams in Pseudomonas aeruginosa. Antimicrob Agents Chemother. 2011;55: 1211–1221. doi:10.1128/AAC.01252-10

41. Zhang L, Mah TF. Involvement of a novel efflux system in biofilm-specific resistance to antibiotics. J Bacteriol. 2008;190: 4447–4452. doi:10.1128/JB.01655-07

42. Quale J, Bratu S, Gupta J, Landman D. Interplay of efflux system, ampC, and oprD expression in carbapenem resistance of Pseudomonas aeruginosa clinical isolates. Antimicrob Agents Chemother. 2006;50: 1633–1641. doi:10.1128/AAC.50.5.1633-1641.2006

43. Pan Y ping, Xu Y hong, Wang Z xin, Fang Y ping, Shen J lu. Overexpression of MexAB-OprM efflux pump in carbapenem-resistant Pseudomonas aeruginosa. Arch Microbiol. Springer Berlin Heidelberg; 2016;198: 565–571. doi:10.1007/s00203-016-1215-7

44. Bolard A, Plesiat P, Jeannot K. Mutations in gene fusA1 as a novel mechanism of aminoglycoside resistance. 2017; 33–3. doi:10.1128/AAC.01835-17

45. López-Causapé C, Rubio R, Cabot G, Oliver A. Evolution of the *Pseudomonas aeruginosa* Aminoglycoside Mutational Resistome In Vitro and in the Cystic

Fibrosis Setting. Antimicrob Agents Chemother. 2018;62: e02583-17. doi:10.1128/AAC.02583-17

46. Acar JF. Antibiotic synergy and antagonism. Med Clin North Am. 2000;84: 1391–1406. doi:https://doi.org/10.1016/S0025-7125(05)70294-7

47. Lehár J, Krueger AS, Avery W, Heilbut AM, Johansen LM, Price ER, et al. Synergistic drug combinations tend to improve therapeutically relevant selectivity. Nat Biotechnol. 2009;27: 659–666. doi:10.1038/nbt.1549

48. Alkawash MA, Soothill JS, Schiller NL. Alginate lyase enhances antibiotic killing of mucoid Pseudomonas aeruginosa in biofilms. Apmis. 2006;114: 131–138. doi:10.1111/j.1600-0463.2006.apm_356.x

49. Moreau-Marquis S, O'Toole GA, Stanton BA. Tobramycin and FDA-approved iron chelators eliminate Pseudomonas aeruginosa biofilms on cystic fibrosis cells. Am J Respir Cell Mol Biol. 2009;41: 305–313. doi:10.1165/rcmb.2008-0299OC

50. Moreau-Marquis S, Coutermarsh B, Stanton BA. Combination of hypothiocyanite and lactoferrin (ALX-109) enhances the ability of tobramycin and aztreonam to eliminate Pseudomonas aeruginosa biofilms growing on cystic fibrosis airway epithelial cells. J Antimicrob Chemother. 2015;70: 160–166. doi:10.1093/jac/dku357

51. Luo J, Dong B, Wang K, Cai S, Liu T, Cheng X, et al. Baicalin inhibits biofilm formation, attenuates the quorum sensing-controlled virulence and enhances Pseudomonas aeruginosa clearance in a mouse peritoneal implant infection model. PLOS One. 2017;12: 1–32.

52. Chait R, Craney A, Kishony R. Antibiotic interactions that select against resistance. Nature. 2007;446: 668–671. doi:10.1038/nature05685

53. Hegreness M, Shoresh N, Damian D, Hartl D, Kishony R. Accelerated evolution of resistance in multidrug environments. Proc Natl Acad Sci. National Academy of Sciences; 2008;105: 13977–13981. doi:10.1073/PNAS.0805965105

54. Baym M, Stone LK, Kishony R. Multidrug evolutionary strategies to reverse antibiotic resistance. Science. 2016;351. doi:10.1126/science.aad3292

55. Maeda T, García-Contreras R, Pu M, Sheng L, Garcia LR, Tomás M, et al. Quorum quenching quandary: resistance to antivirulence compounds. ISME J. 2012;6: 493–501. doi:10.1038/ismej.2011.122

56. Wale N, Sim DG, Jones MJ, Salathe R, Day T, Read AF. Resource limitation prevents the emergence of drug resistance by intensifying within-host competition. Proc Natl Acad Sci. 2017; 201715874. doi:10.1073/pnas.1715874115

57. Mellbye B, Schuster M. The sociomicrobiology of antivirulence drug resistance: a proof of concept. MBio. 2011;2: e00131-11. doi:10.1128/mBio.00131-11

58. Gerdt JP, Blackwell HE. Competition Studies Confirm Two Major Barriers That Can Preclude the Spread of Resistance to Quorum-Sensing Inhibitors in Bacteria. ACS Chem Biol. 2014;9: 2291–2299. doi:10.1021/cb5004288

59. Vega NM, Gore J. Collective antibiotic resistance: Mechanisms and implications. Curr Opin Microbiol. Elsevier Ltd; 2014;21: 28–34. doi:10.1016/j.mib.2014.09.003

60. Fischbach MA. Combination therapies for combating antimicrobial resistance. Curr Opin Microbiol. Elsevier Ltd; 2011;14: 519–523. doi:10.1016/j.mib.2011.08.003

61. Silver LL. Challenges of Antibacterial Discovery. Clin Microbiol Rev. 2011;24:

775 71–109. doi:10.1128/CMR.00030-10

776 62. Tepekule B, Uecker H, Derungs I, Frenoy A, Bonhoeffer S. Modeling antibiotic
777 treatment in hospitals: A systematic approach shows benefits of combination
778 therapy over cycling, mixing, and mono-drug therapies. PLOS Comput Biol.
779 2017;13: 1–22. doi:10.1371/journal.pcbi.1005745

780 63. Tyers M, Wright GD. Drug combinations: a strategy to extend the life of
781 antibiotics in the 21st century. Nat Rev Microbiol. Springer US; 2019;17: 141–
782 155. doi:10.1038/s41579-018-0141-x

783 64. Bayat Mokhtari R, Homayouni TS, Baluch N, Morgatskaya E, Kumar S, Das B,
784 et al. Combination therapy in combating cancer. Oncotarget. United States;
785 2017;8: 38022–38043. doi:10.18632/oncotarget.16723

786 65. Cihlar T, Fordyce M. Current status and prospects of HIV treatment. Curr Opin
787 Virol. 2016;18: 50–56. doi:https://doi.org/10.1016/j.coviro.2016.03.004

788 66. Ginsberg AM, Spigelman M. Challenges in tuberculosis drug research and
789 development. Nat Med. United States; 2007;13: 290–294.
790 doi:10.1038/nm0307-290

791 67. Zhou L, Slamti L, Nielsen-LeRoux C, Lereclus D, Raymond B. The Social
792 Biology of Quorum Sensing in a Naturalistic Host Pathogen System. Curr Biol.
793 Cell Press; 2014;24: 2417–2422. doi:10.1016/J.CUB.2014.08.049

794 68. Rezzoagli C, Granato E, Kuemmerli R. In vivo microscopy reveals the impact
795 of Pseudomonas aeruginosa social interactions on host colonization. ISME J.
796 2019;

797 69. Choi K-H, Schweizer HP. mini-Tn7 insertion in bacteria with single attTn7 sites:
798 example *Pseudomonas aeruginosa*. Nat Protoc. 2006;1: 153–161.
799 doi:10.1038/nprot.2006.24

800 70. Kümmerli R, Jiricny N, Clarke LS, West SA, Griffin AS. Phenotypic plasticity of
801 a cooperative behaviour in bacteria. J Evol Biol. 2009;22: 589–598.
802 doi:10.1111/j.1420-9101.2008.01666.x
803 71. Özkaya Ö, Balbontín R, Gordo I, Xavier KB. Cheating on Cheaters Stabilizes
804 Cooperation in *Pseudomonas aeruginosa*. Curr Biol. 2018;26: 2070–2080.
805 doi:10.1016/j.cub.2018.04.093
806 72. Ocampo PS, Lázár V, Papp B, Arnoldini M, Zur Wiesch PA, Busa-Fekete R, et
807 al. Antagonism between bacteriostatic and bactericidal antibiotics is prevalent.
808 Antimicrob Agents Chemother. 2014;58: 4573–4582. doi:10.1128/AAC.02463-
809 14
810 73. Rezzoagli C, Wilson D, Weigert M, Wyder S, Kümmerli R. Probing the
811 evolutionary robustness of two repurposed drugs targeting iron uptake in
812 *Pseudomonas aeruginosa*. Evol Med Public Heal. 2018;1: 246–259.
813 doi:10.1093/emph/eoy026
814 74. Morones-Ramirez JR, Winkler JA, Spina CS, Collins JJ. Silver Enhances
815 Antibiotic Activity Against Gram-Negative Bacteria. Sci Transl Med. 2013;5: 1–
816 12.
817 75. Baeder DY, Yu G, Hozé N, Rolff J, Regoes RR. Antimicrobial combinations:
818 Bliss independence and Loewe additivity derived from mechanistic multi-hit
819 models. Philos Trans R Soc B Biol Sci. 2016;371. Available:
820 http://rstb.royalsocietypublishing.org/content/371/1695/20150294.abstract
821 76. Barbosa C, Beardmore R, Schulenburg H, Jansen G. Antibiotic combination
822 efficacy (ACE) networks for a Pseudomonas aeruginosa model. PLOS Biol.
823 2018;16: 1–25.
824 77. Bolger AM, Lohse M, Usadel B. Trimmomatic: a flexible trimmer for Illumina

825 sequence data. Bioinformatics. 2014;30: 2114–2120.
826 doi:10.1093/bioinformatics/btu170
827 78. Danecek P, Auton A, Abecasis G, Albers CA, Banks E, DePristo MA, et al. The
828 variant call format and VCFtools. Bioinformatics. 2011/06/07. Oxford University
829 Press; 2011;27: 2156–2158. doi:10.1093/bioinformatics/btr330
830 79. Ross-Gillespie A, Gardner A, West SA, Griffin AS. Frequency dependence and
831 cooperation: theory and a test with bacteria. Am Nat. 2007;170: 331–342.
832 doi:10.1086/519860
833 80. R Development Core Team. R: A language and environment for statistical
834 computing. R Foundation for Statistical Computing. Vienna, Austria; 2013.
835 81. Ritz C, Baty F, Streibig JC, Gerhard D. Dose-Response Analysis Using R.
836 PLOS One. 2015;10: 1–13. doi:10.1371/journal.pone.0146021
837 82. Higgins PG, Fluit AC, Milatovic D, Verhoef J, Schmitz FJ. Mutations in GyrA,
838 ParC, MexR and NfxB in clinical isolates of Pseudomonas aeruginosa. Int J
839 Antimicrob Agents. 2003;21: 409–413. doi:10.1016/S0924-8579(03)00009-8
840 83. Miller AK, Brannon MK, Stevens L, Johansen HK, Selgrade SE, Miller SI, et al.
841 PhoQ mutations promote lipid A modification and polymyxin resistance of
842 Pseudomonas aeruginosa found in colistin-treated cystic fibrosis patients.
843 Antimicrob Agents Chemother. 2011;55: 5761–5769. doi:10.1128/AAC.05391-
844 11
845 84. Lee JY, Park YK, Chung ES, Na IY, Ko KS. Evolved resistance to colistin and
846 its loss due to genetic reversion in Pseudomonas aeruginosa. Sci Rep. Nature
847 Publishing Group; 2016;6: 1–13. doi:10.1038/srep25543
848 85. Barrow K, Kwon DH. Alterations in two-component regulatory systems of
849 phoPQ and pmrAB are associated with polymyxin B resistance in clinical

isolates of Pseudomonas aeruginosa. Antimicrob Agents Chemother. 2009;53: 5150–5154. doi:10.1128/AAC.00893-09

86. Sanz-garcía F, Hernando-amado S, Martínez L. Mutation-Driven Evolution of Pseudomonas aeruginosa in the Presence of either Ceftazidime or Ceftazidime-Avibactam. Antimicrob Agents Chemother. 2018;62: e01379-18.

87. Winsor GL, Griffiths EJ, Lo R, Dhillon BK, Shay JA, Brinkman FSL. Enhanced annotations and features for comparing thousands of Pseudomonas genomes in the Pseudomonas genome database. Nucleic Acids Res. 2015;44: D646–D653. doi:10.1093/nar/gkv1227

88. Kahm M, Hasenbrink G, Ludwig J. grofit: Fitting Biological Growth Curves with R. J Stat Softw. 2010;33: 1–21. doi:10.18637/jss.v033.i07

Figures

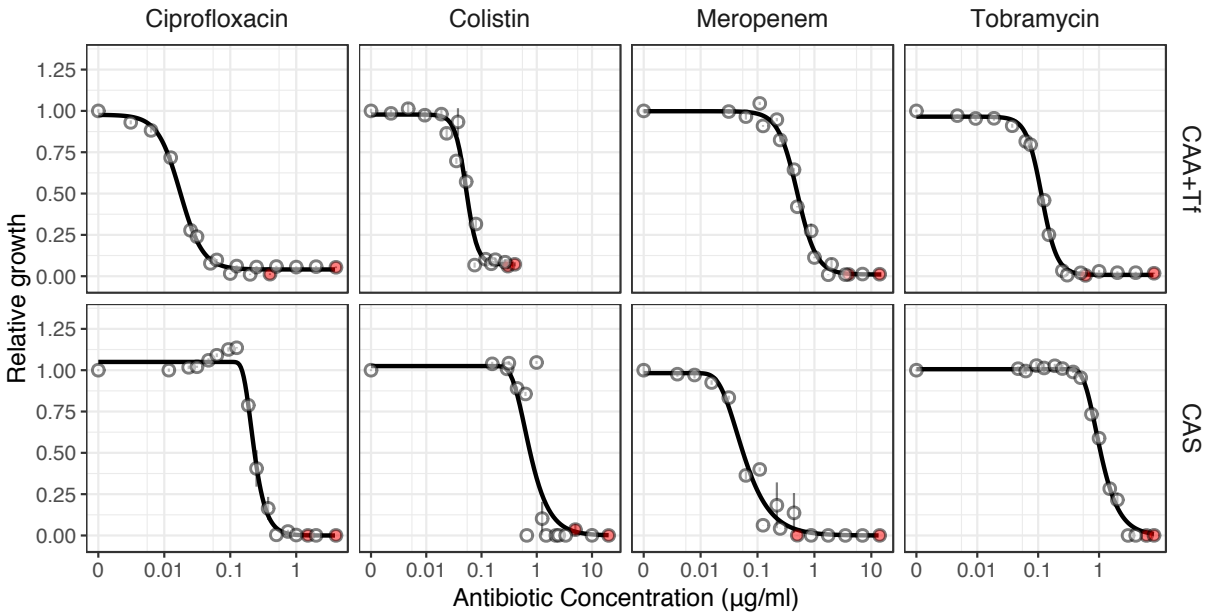

Figure 1. Antibiotic dose response curves for *P. aeruginosa* PAO1 populations. We exposed PAO1 to all four antibiotics in two experimental media: CAA+Tf (iron-limited casamino acids medium with transferrin) and CAS (casein medium). Except for meropenem, higher concentrations of antibiotics were required to inhibit PAO1 in CAS compared to CAA+Tf. Dots show means ± standard error across six replicates. All data are scaled relative to the drug-free treatment. Data stem from two independent experiments using different dilution series. The red dots indicate the highest concentration used for the respective experiments, from which 7-serial dilution steps were tested. Curves were fitted with either log-logistic functions (in CAA+Tf) or with three-parameter Weibull functions (in CAS).

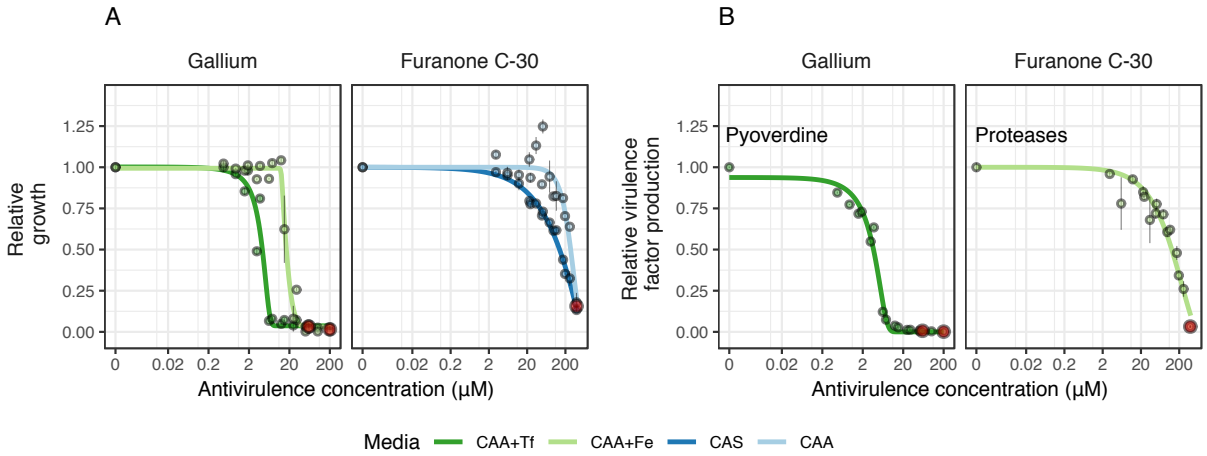

874

875 **Figure 2. Antivirulence dose response curves for *P. aeruginosa* PAO1**
876 **populations (growth and virulence factor production)**. We exposed PAO1 to the
877 antivirulence compounds gallium (inhibiting pyoverdine-mediated iron uptake) and
878 furanone C-30 (blocking quorum sensing response including protease production) both
879 in media where the targeted virulence factors are expressed and required (iron-limited
880 CAA+Tf medium for gallium and CAS medium for furanone) and in control media
881 where the targeted virulence factors are not required (iron-supplemented CAA+Fe
882 medium for gallium and protein digested CAA for furanone). (**A**) Dose-response curves
883 for growth show that both antivirulence compounds reduced bacterial growth, but more
884 so in media where the targeted virulence factor is expressed. This demonstrates that
885 there is a concentration window where the antivirulence compounds have no toxic
886 effects on bacterial cells and just limit growth due to virulence factor quenching. (**B**)
887 Dose-response curves for virulence factor production show that gallium and furanone
888 C-30 effectively inhibit pyoverdine and protease production, respectively, in a
889 concentration-dependent manner. Dots show means ± standard errors across six
890 replicates. All data are scaled relative to the drug-free treatment. Data stem from two
891 independent experiments using different dilution series. The red dots indicate the
892 highest concentration used for the respective experiments, from which 7-serial dilution
893 steps were tested. Curves were fitted with either log-logistic functions (in CAA+Tf) or
894 with three-parameter Weibull functions (in CAS).

895

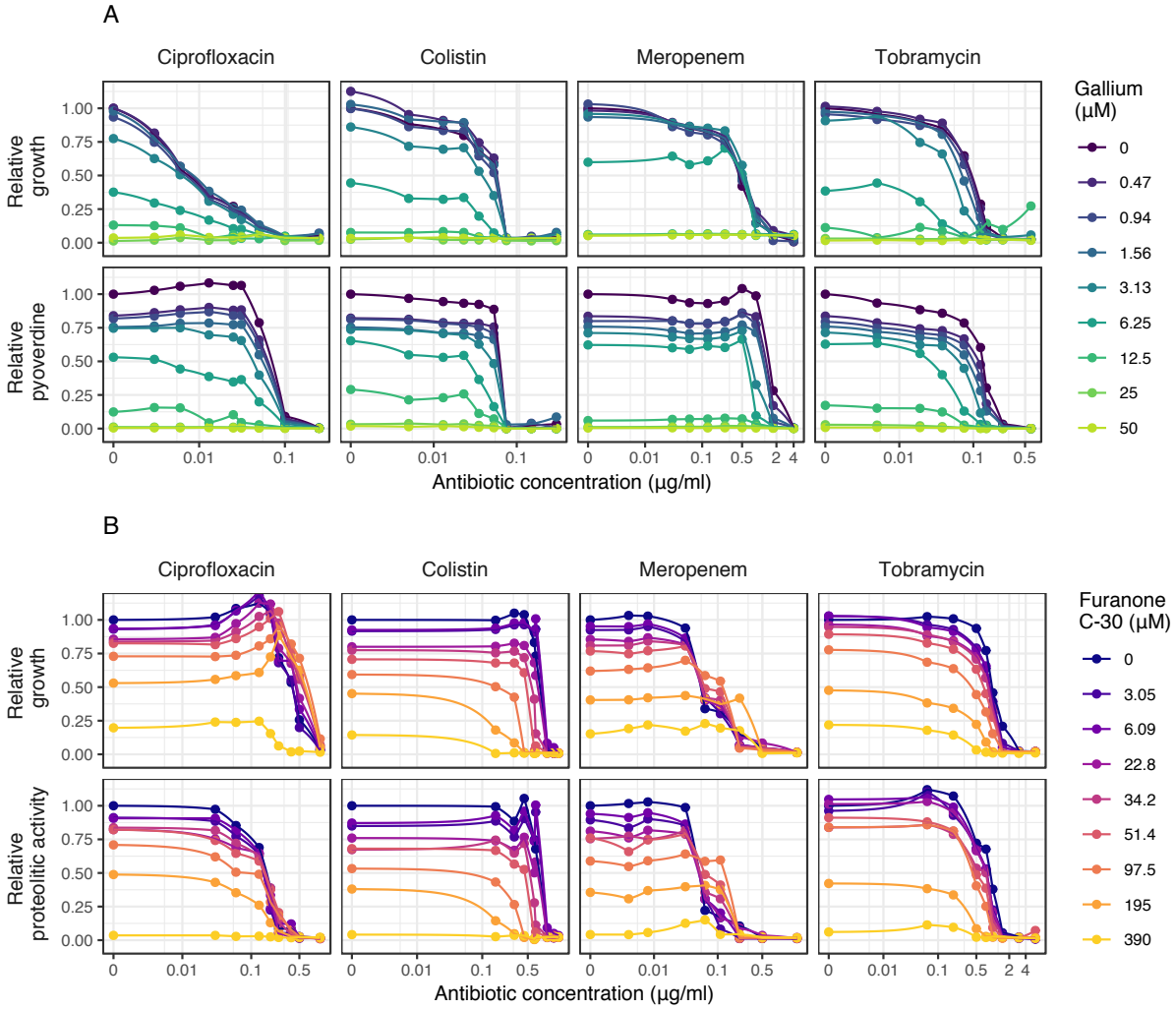

Figure 3. Dose response curves for *P. aeruginosa* PAO1 populations under antibiotic-antivirulence combination treatments. Dose-response curves for growth and virulence factor production for PAO1 were assessed for 9x9 drug concentration matrixes involving the four antibiotics combined with either gallium (**A**) or furanone C-30 (**B**). Experiments were carried out in media where the corresponding virulence factors are required for growth (pyoverdine: CAA+Tf; protease: CAS). Growth and virulence factor production were measured after 48 hours. All values are scaled relative to the untreated control, and data points show the mean across 12 replicates from two independent experiments. We used spline functions to fit the dose-response curves.

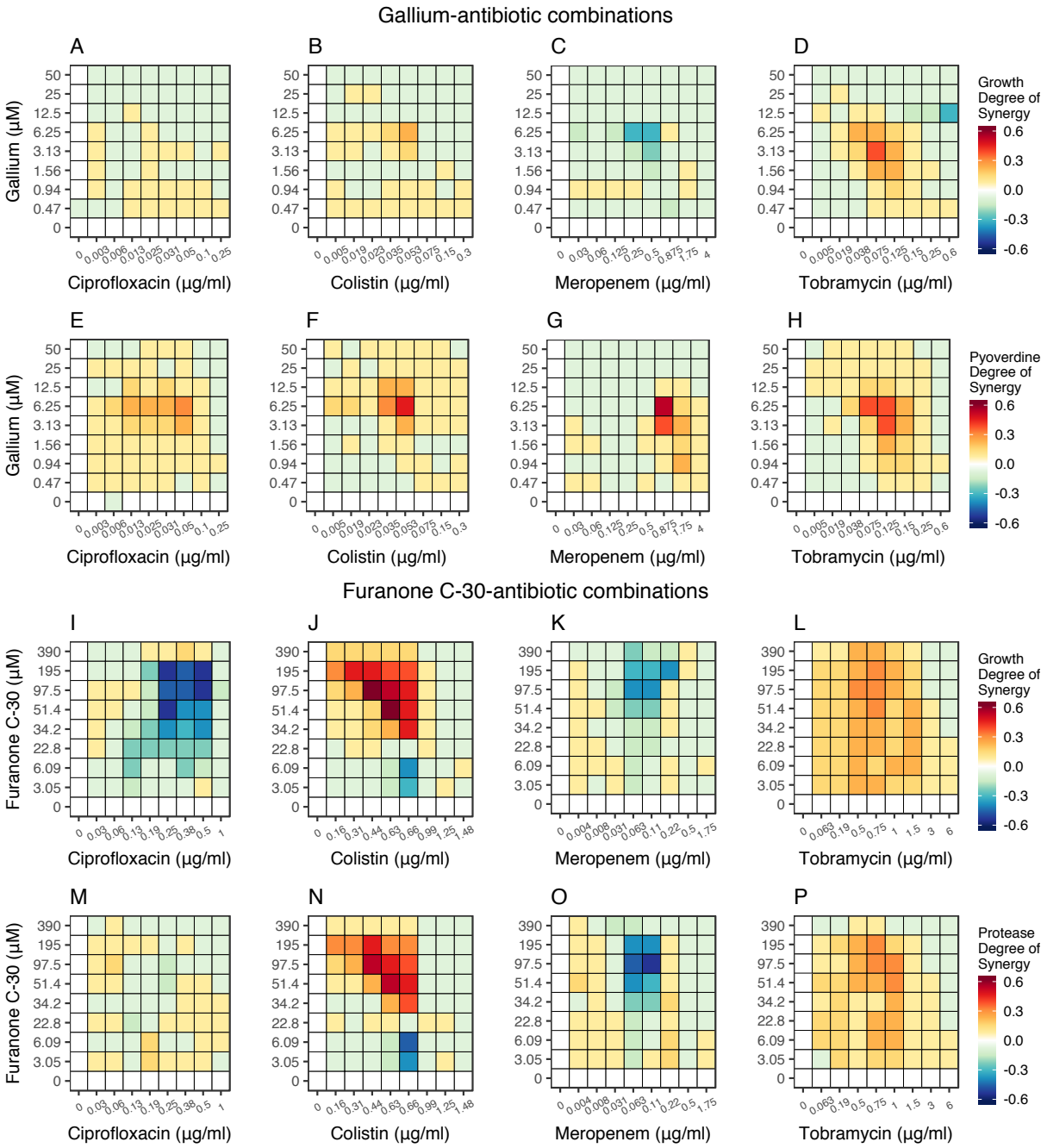

Figure 4: Drug interaction heatmaps for antibiotic-antivirulence combination treatments. We used the Bliss independence model to calculate the degree of synergy for every single drug combination with regard to growth suppression and virulence factor quenching shown in Figure 3. Heatmaps, depicting variation in drug interactions ranging from antagonism (blue) to synergy (red), are shown for gallium-antibiotic combinations (**A-D** for growth; **E-H** for pyoverdine production) and furanone-antibiotic combinations (**I-L** for growth; **M-P** for protease production). All calculations are based on 12 replicates from two independent experiments.

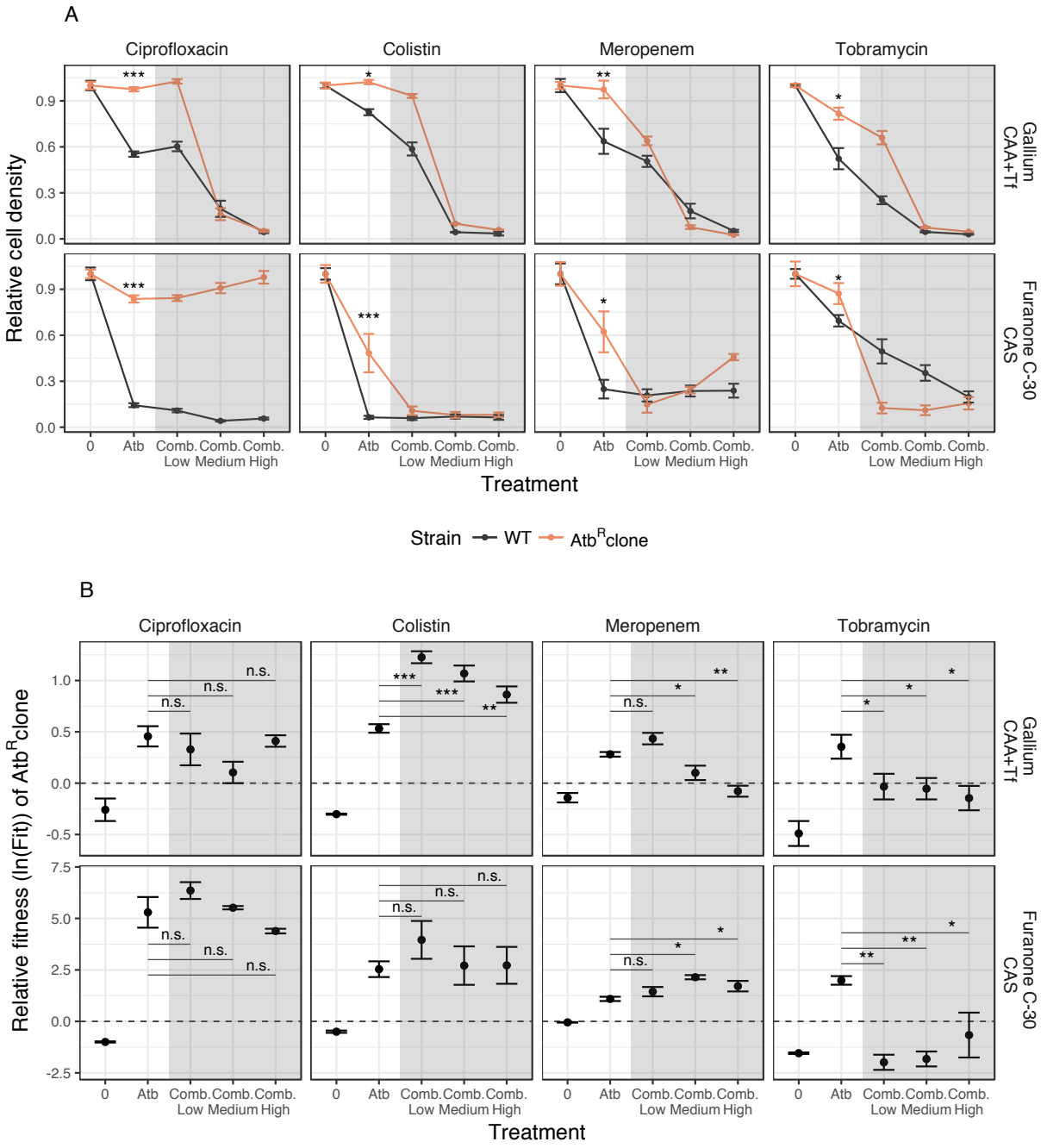

Figure 5: Effect of combination treatment on the fitness of antibiotic resistant clones. (**A**) Test of whether the addition of antivirulence compounds can restore growth suppression in antibiotic resistant clones (AtbR, in orange) relative to the susceptible wildtype (WT, in black). Under antibiotic treatment and in the absence of antivirulence compounds, all AtbR strains grow significantly better than the WT, a result that holds for both scaled (as shown above) and absolute growth. In the presence of antivirulence compounds (gray shaded area), growth suppression was restored in seven out of eight drug combinations (except for the furanone-ciprofloxacin combo). Antivirulence compound concentrations used for gallium: 1.56 μM (combo

low), 6.25 µM (combo medium), 12.5 µM (combo high); for furanone C-30: 6.1 µM (combo low), 22.8 µM (combo medium), 51.4 µM (combo high). Important to note is that all antivirulence compound concentrations do not or only mildly affect pathogen growth when applied as single treatments (Figure 2). All cell density values (measured with flow cytometry as number of events detected in 5 µl of culture, after 24 hours) are scaled relative to the untreated control. (**B**) Test of whether the addition of antivirulence compounds can revert selection for antibiotic resistance during competition between AtbR and WT, starting at a 1:9 ratio. The dashed lines denote fitness parity, where none of the competing strains has a fitness advantage. With no treatment, all AtbR strains showed a fitness disadvantage (fitness values < 0) compared to the WT. When treated with antibiotics alone, all AtbR strains experienced significant fitness advantages. When antivirulence compounds were added as adjuvants, this fitness advantage was lost for three drug combinations: meropenem-gallium, tobramycin-gallium, tobramycin-furanone C-30, thus showing reversal of AtbR selection. All data are shown as means ± standard errors across a minimum of eight replicates from two to three independent experiments. Significance levels are based on ANOVAs: n.s. = non-significant; * $p < 0.05$; ** $p < 0.01$; *** $p < 0.001$. See Supplementary Table S3 for details on statistical analysis.

946 **Table 1. List of mutations in the antibiotic resistant clones**

AtbR clone[a,b]	Combination with	Gene[c]	Description	Mutation type[b]	Reference	Variant	Position[d]	Reference
CpR_1	Gallium Furanone C-30	*gyrB*	DNA gyrase subunit B	INDEL	CCCAGGAG	CG	5671	[36]
		mexR	Multidrug resistance operon repressor	INDEL	ATCAGTGCCT TGTCGCGGCA	AA	471547	[37,82]
CoR_1	Gallium	*phoQ*	Two-component sensor PhoQ	SNP	T	G	1279140	[38,83–85]
CoR_2	Furanone C-30	*phoQ*	Two-component sensor PhoQ	INDEL	T	TC	1279085	[38,83–85]
				SNP	T	C	1279089	
		PA1327	Probable protease	INDEL	CA	C	1440622	
MeR_1	Gallium	*mpl*	UDP-N-acetylmuramate:L-alanyl-gamma-D-glutamyl-meso-diaminopimelate ligase	SNP	T	G	4499740	[39,86]
MeR_2	Furanone C-30	*parR*	Two-component response regulator, ParR	SNP	C	T	1952257	[40]
		PA1874	Hypothetical protein (efflux pump)	COMPLEX	ACCGGG	CCCGTC	2039326	[41]
				SNP	A	G	2039485	
				SNP	C	T	2039494	
				SNP	T	C	2039512	
				SNP	G	A	2039517	
				SNP	T	C	2039524	

				COMPLEX	CGGG	TGGC	2039530	
		nalD	Transcriptional regulator NalD	SNP	A	C	4006981	[42,43]
TbR_1	Gallium	*fusA1*	Elongation factor G	SNP	C	T	4769121	[44]
				SNP	T	G	5253694	
TbR_2	Furanone C-30	*fusA1*	Elongation factor G	SNP	T	C	4770785	[44]
		pscP	Translocation protein in type III secretion system	INDEL	$TG(TTGGCG)_{x11}$	$TG(TTGGCG)_{x12}$	1844903	
		PA4132	Conserved hypothetical protein	SNP	A	C	4621443	

947

948 [a]The antibiotic resistant strains are referred to as AtbR throughout the text.

949 [b]Abbreviations: Atb: antibiotic; Cp: ciprofloxacin; Co: colistin; Me: meropenem; Tb: tobramycin; SNP: single nucleotide polymorphism;
950 INDEL: insertion or deletion; COMPLEX: multiple consecutive SNPs .

951 [c]Mutations in the ancestor wildtype background compared to the reference PAO1 genome are reported in [73].

952 [d]Position on PAO1 reference genome [87].